EASR

Engineering and Applied Science Research

https://www.tci-thaijo.org/index.php/easr/index

Published by the Faculty of Engineering, Khon Kaen University, Thailand

Comparison of artificial neural network and response surface methodology in predicting the tensile strength and optimization of 3D printed objects

Pichai Janmanee and Pongpun Ratchapakdee*

Department of Industrial Engineering, Faculty of Engineering, Rajamangala University of Technology Krungthep, Bangkok, Thailand

Received 1 March 2024
Revised 29 September 2024
Accepted 29 October 2024

Abstract

This study investigates the geometric properties of 3D-printed objects using fused deposition modelling. It focuses on optimising parameters for printing in terms of their significant impact on both the quality and cost of printed objects. To enhance the quality of 3D-printed objects, it is crucial to predict the geometric properties in advance. The development of an artificial neural network model (ANN) is employed to predict the tensile strength properties of polylactic acid material during experiments. The model considers three variables: printing temperatures at three levels (190°C, 210°C, and 230°C), printing speeds at three levels (30 mm/s, 50 mm/s, and 70 mm/s), and material infill density at three levels (40%, 60%, and 80%). Tensile strength testing was conducted, and the predictive performance of ANN models was compared with mathematical models derived from the application of response surface methodology (RSM). The goal was to determine suitable printing conditions. Tensile strength testing revealed that printing temperature, printing speed, and infill density significantly impact tensile strength. The ANN configuration consists of a 3-input layer with 3 neurons, a hidden layer with 14 neurons, and an output layer with 1 neuron, denoted as 3-14-1. The model exhibited a testing decision-making accuracy of 0.938. The average error for the ANN model was 0.307, lower than the average error from the full factorial model, which was 1.392. The optimized printing conditions for maximum tensile strength were found to be a print temperature (X_1) of 230°C, a feed rate (X_2) of 30 mm/sec, and an infill density (X_3) of 80%, resulting in a tensile strength of 43.107 MPa. The mathematical model derived from RSM demonstrated efficacy in predicting and controlling the quality of printed objects, aiming to reduce production costs and enhance efficiency in future 3D printing processes.

Keywords: Fused deposition modelling, Prediction, Response surface methodology, Artificial neural network, Tensile strength

1. Introduction

Three-dimensional printing (3D Printing) is a process of creating three-dimensional shapes following the principles of additive manufacturing. The objective is to produce rapid prototypes. Shapes are generated from computer model data using software to define various parameters in a layered stacking format. The printing process involves building up the object layer by layer, either in a horizontal plane or cross-section, starting from the base and progressing to the top of the object [1]. This method enables the creation of freely shaped and complex objects without the need for moulds. Since it involves creating an object directly from the initial material, almost 100%, without cutting, drilling, or subtracting material, it reduces costs [2]. This technology has rapidly evolved, leading to the emergence of numerous innovative printing techniques. The advantages of 3D printing include the ability to produce complex shapes in a short period [3]. Currently, Fused Deposition Modelling (FDM) is a widely used 3D printing technology due to its cost-effectiveness compared to other techniques as well as its ease of use and maintenance [4]. FDM is a rapid prototyping technology found in various applications, including the aerospace, automotive, medical equipment, and food industries. It is also known for using safe printing materials [5]. Fused deposition modelling (FDM) is one of several three-dimensional (3D) printing techniques that employ flexible thermoplastic filaments injected through a heated nozzle to build components [6]. The thermoplastics and reinforced thermoplastic materials that can be printed with FDM include acrylonitrile butadiene styrene (ABS), polylactic acid (PLA), polycarbonate, unfilled polyetherimide (PEI), Polyether ether ketone (PEEK), Polyethylene terephthalate glycol (PETG) [7], and fibre-reinforced thermoplastics [8, 9]. FDM-produced components are indeed gaining prominence and replacing conventional components in various industries, notably in the automotive, aviation, and medical sectors [10, 11]. The process variables and their settings have a substantial impact on the mechanical qualities of FDM-printed components [12]. As a result, enhancing the mechanical qualities of printed components requires analysing the effects of input factors and anticipating results by using adequate settings [13]. Artificial Neural Network (ANN) models have gained widespread acceptance in artificial intelligence (AI) research for simulating the workings of the human brain to make predictions based on data. The advantages of ANN models include their ability to automatically extract special features from input data [14]. This is in contrast to traditional machine learning approaches where feature extraction requires manual intervention, leading to the possibility of errors [15]. Currently, artificial neural networks (ANNs) are being applied extensively

*Corresponding author.
Email address: 649041610035@mail.rmutk.ac.th; r_pongpun@hotmail.com
doi: 10.14456/easr.2024.66

in various fields, including predicting the mechanical properties of 3D-printed objects. Research studies [16-18] have examined the impact of parameters in the Fused Deposition Modelling (FDM) printing process on the tensile strength of materials such as ABS, PETG, and samples with multiple materials. The study employed artificial neural networks (ANNs) and the Genetic Algorithm-Artificial Neural Network (GA-ANN) in MATLAB-16.0 to train datasets for optimising process parameters. The study investigated the effects of layer height, build angle, and post-curing time on the dimensional accuracy and surface roughness of 3D-printed specimens made of digital light processing resin. In addition, MOGA-ANN was employed to maximise the output responses and reach 97.84% dimensional accuracy. Using the potential of MOGA-ANN optimization, manufacturers and researchers may produce high-quality, dependable, and biocompatible 3D-printed components, paving the way for innovative medical devices and personalised healthcare solutions [19].

This research focused on three variables, including material density, infill density, and compression moulding temperature. The experimental results revealed that the compression moulding temperature and material infill density significantly affect the tensile strength. Tensile strength is more influenced by the compression moulding temperature than the material infill density. The predicted values closely matched the experimental results. Additionally, a study was conducted to develop a model using Artificial Neural Network (ANN) to predict the impact of key factors in the fused deposition modelling (FDM) process on the quality of Acrylonitrile Butadiene Styrene (ABS) printed parts. The experimental design followed the Taguchi L9 approach, with varying parameters such as layer thickness, build orientation angle, and support structure angle. The ANN model was used to predict the mathematical impact of different print settings on surface roughness during the use of ABS material. The model accurately predicted the maximum deviation of 4.664 per cent from the average mathematical surface roughness (Ra), demonstrating its capability to forecast the impact of various print settings on surface quality [20]. From past research, it has been identified that there is a lack of studies focusing on a comparative analysis of tensile strength values obtained from experimental design against the development of artificial network (ANN) models for polylactic acid (PLA) 3D-printed objects using the fused deposition modelling (FDM) process.

Additionally, the selection of appropriate printing conditions is crucial for developing tools to aid in the selection of factors. The levels of factors that significantly influence the tensile strength values need to be determined. Key input factors for consideration include printing temperature, print speed, and material infill density, as these factors have a substantial impact on the mechanical properties and microstructure [21, 22]. The output variable in this research is the tensile strength value. Therefore, the study applies the design of experiment (DOE) method to design experiments for surface response and create a mathematical model for predicting tensile strength values. Subsequently, the performance of this model is compared with predictions obtained from an artificial neural network (ANN) model. Additionally, the study aims to determine the appropriate conditions. The developed model can be applied to forecast tensile strength values, contributing to cost reduction in 3D printing and enhancing the efficiency of 3D-printed objects in future applications. The methodologies that will be applied to the suggested research are shown in Figure 1.

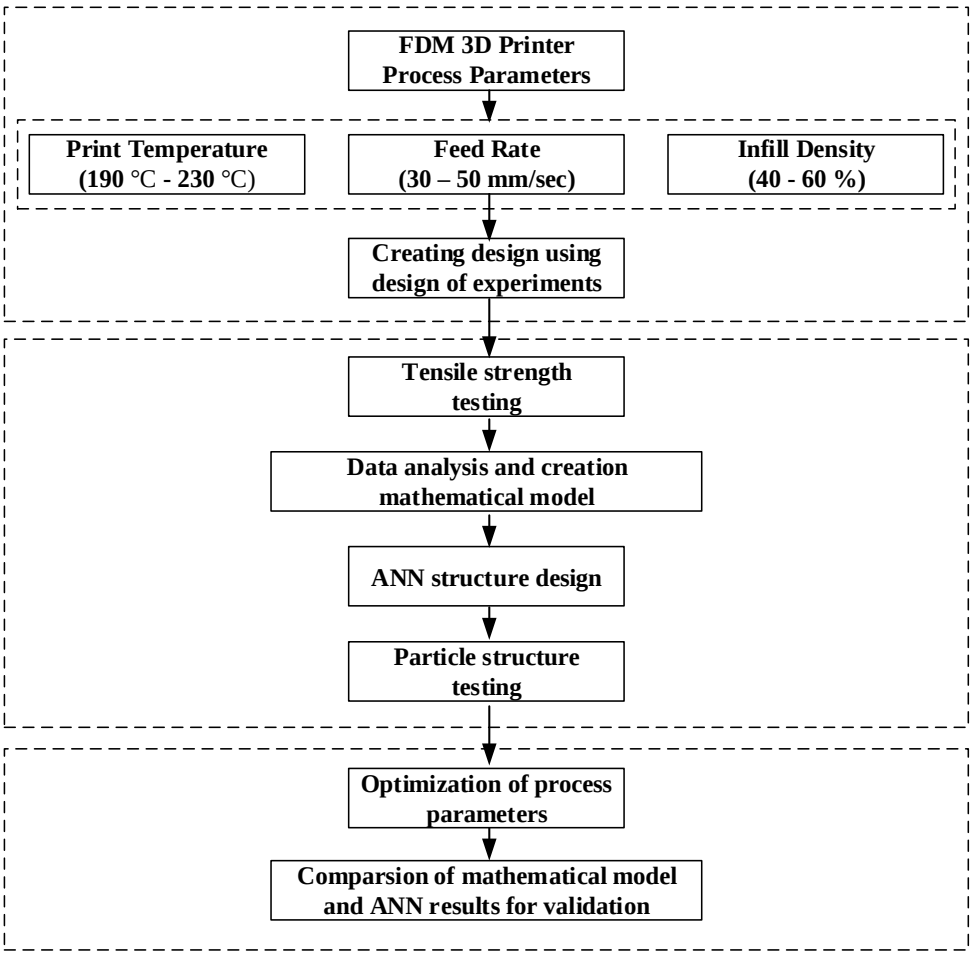

Figure 1 A flowchart of the methodology employed in the proposed research

2. Materials and methods

2.1 Materials used in the research

The plastic filament used for experimentation was polylactic acid (PLA) from the brand E-sun, with a diameter of 1.75 mm.

2.2 Preparation of test specimens

Test specimens were 3D printed using a fused deposition modelling (FDM) 3D printer, specifically the Ender 5 Pro model, with a nozzle diameter of 0.4 mm. The printing parameters were set to a bed temperature of 60°C and a layer thickness of 0.2 mm. The printing pattern used was a straight-line pattern, and specimens were printed in the +45°/45° orientation [23].

2.3 Experimental design

The research defined three factors for study: print temperature, feed rate, and infill density. These factors were chosen because they significantly impact the adhesion and cooling rates of each layer, and result in stringing and voids in the printed object if improperly selected, affecting both the mechanical properties and structure [24]. The study applied the surface response methodology to create mathematical models and artificial neural network models using MATLAB software. Additionally, suitable factor levels were determined. The experimental design involved three levels for each factor, and the experiments were conducted with three replications, as shown in Table 1.

Table 1 Experimental Design Variables

Factor	Level			Unit
Print Temperature (X_1)	190	210	220	(°C)
Feed Rate (X_2)	30	50	70	(mm/sec)
Infill Density (X_3)	40	60	100	(%)

2.4 Tensile strength testing

The tensile strength testing utilised test specimens designed using SolidWorks software, as shown in Figure 2. The layering of the specimen was accomplished using Creality software. Testing was conducted using a SHIMADZU Universal Testing Machine AGS-X model 100 kN, as depicted in Figure 3. The test speed was set to 5 mm/min following the ASTM D368 standard [25].

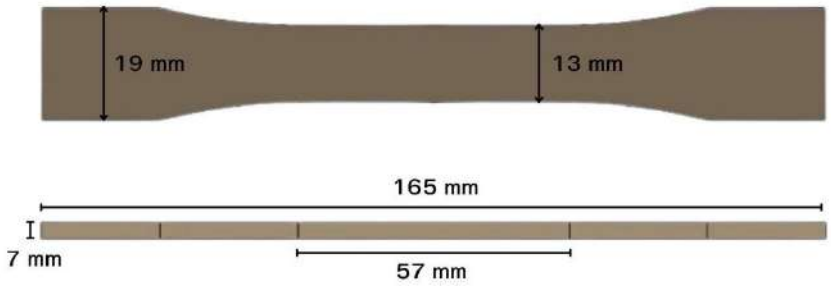

Figure 2 Tensile test specimen according to ASTM D638 standard

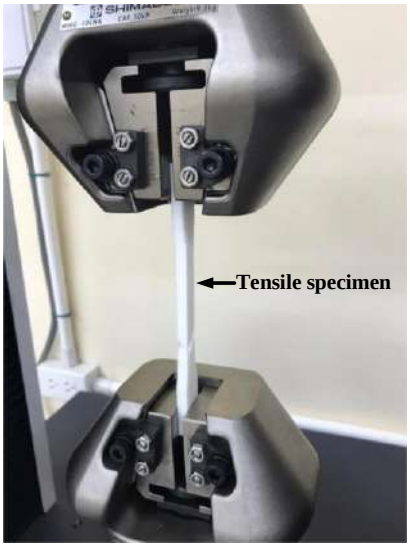

Figure 3 Tensile test

2.5 Particle structure testing

After printing the specimens, the surfaces were prepared by examining the particle structure of the specimens using a scanning electron microscope (SEM).

2.6 ANN structure design

Artificial neural networks (ANN) have gained widespread acceptance in non-linear artificial intelligence (AI) research. ANN is a computational model that mimics the functioning of the human brain to benefit from data prediction. It consists of neural cells that simulate the workings of the human brain, using transfer functions (f), weights (w), and biases (b) as tools to model the properties of neural cells [26]. The research employed a multi-layer neural network to build the artificial neural network model. The input factors, print temperature, feed rate, and infill density were determined through the designed experiment using the response surface methodology. The output factor was the tensile resistance value. Various model structures were designed and tested, and model performance was evaluated. The results were summarised, and the best-performing model was selected based on the mean square error, as displayed in Figure 4.

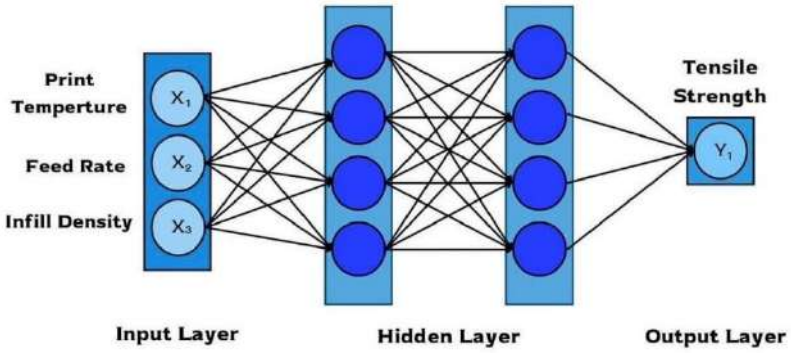

Figure 4 Multi-layer neural network model

2.6.1 Data formatting for training and testing

For the training and testing processes, data formatting was organised based on three input factors and one output target from the experimental results obtained through the response surface methodology. The analysis involved a dataset with 1,000 epochs. In this research, cross-validation was employed, specifically utilising the K-fold cross-validation technique, to evaluate the model's predictive error. The data were divided equally into three sets, each comprising 27 data points. Two sets were used for the training process, and the remaining set was reserved for testing. The testing phase was conducted over three rounds.

2.6.2 Designing a suitable neural network structure

The neural network structure in this research involved dividing the data for training and testing to facilitate learning through the backpropagation technique. The training utilised the Levenberg-Marquardt Algorithm [14], and the learning function employed the learning gradient descent (Learngd). The activation functions chosen were the log-sigmoid for the input layer, the tan-sigmoid for the hidden layer, and purelin for the output layer. The models were iterated for 1,000 epochs. The transfer functions can be calculated using equations (1)-(3) [17].

$$a = Logsig(n) = \frac{1}{1+e^{n}} \quad (1)$$

$$a = Logsig(n) = \frac{1}{1+e^{-n}} \quad (2)$$

$$a = Purelin(n) \quad (3)$$

The process of constructing the artificial neural network (ANN) model involved defining three input factors: print temperature, feed rate, and infill density. The experimental design for the surface response method was developed, considering the export factor of tensile resistance. Subsequently, various model structures were designed, encompassing a single layer with six distinct configurations, each differing in the number of neurons based on the mean square error (MSE) values. Following this, the designed models were tested to determine the most efficient configuration, aiming for the lowest average squared error. 3.3) Evaluation of the performance of the neural network model was conducted based on the mean square error (MSE) and decision coefficient (R^2) values, as illustrated in Equations (4) and (5) [17]. The mean square error (MSE) is as follows:

$$MSE = \frac{\sum_{i=1}^{N}(T_i - A_i)^2}{N} \quad (4)$$

For the neural network model, the consideration of the coefficient of determination (R^2) is expressed by the following equation:

$$R^2 = 1 - \frac{\sum_{i=1}^{N}(T_i - A_i)^2}{\sum_{i=1}^{N}(T_i - A_i)^2} \quad (5)$$

Where: T is the target result.
A is the result obtained from prediction.
N is the number of data points.

2.7 Comparison of performance testing between artificial neural network model and mathematical model

The predictive performance of the tensile resistance values for 3D-printed objects was compared using both the mathematical model obtained from the surface response experiment and the model derived from the utilisation of the neural network. Subsequently, the model that demonstrates accurate predictions for tensile resistance values based on the mean square error (MSE) average is selected. The chosen model can be applied to predict tensile resistance values, contributing to cost reduction in 3D printing and facilitating effective production planning. This enhances overall efficiency in the production of three-dimensional printed objects moving forward.

3. Results

3.1 Experimental results using response surface methodology

In this research, the response surface methodology (RSM) was employed as an experimental design approach, including the creation of a mathematical model for predicting tensile resistance values. Subsequently, the predictive capabilities of the selected mathematical model were compared to those of the neural network-derived model. The appropriate mathematical model obtained from the response surface methodology, found to be suitable for accurate predictions, is the full quadratic equation model. The analysis of the data was performed with this model, employing a 95% confidence level and a P-value of 0.05. The research findings are detailed as follows:

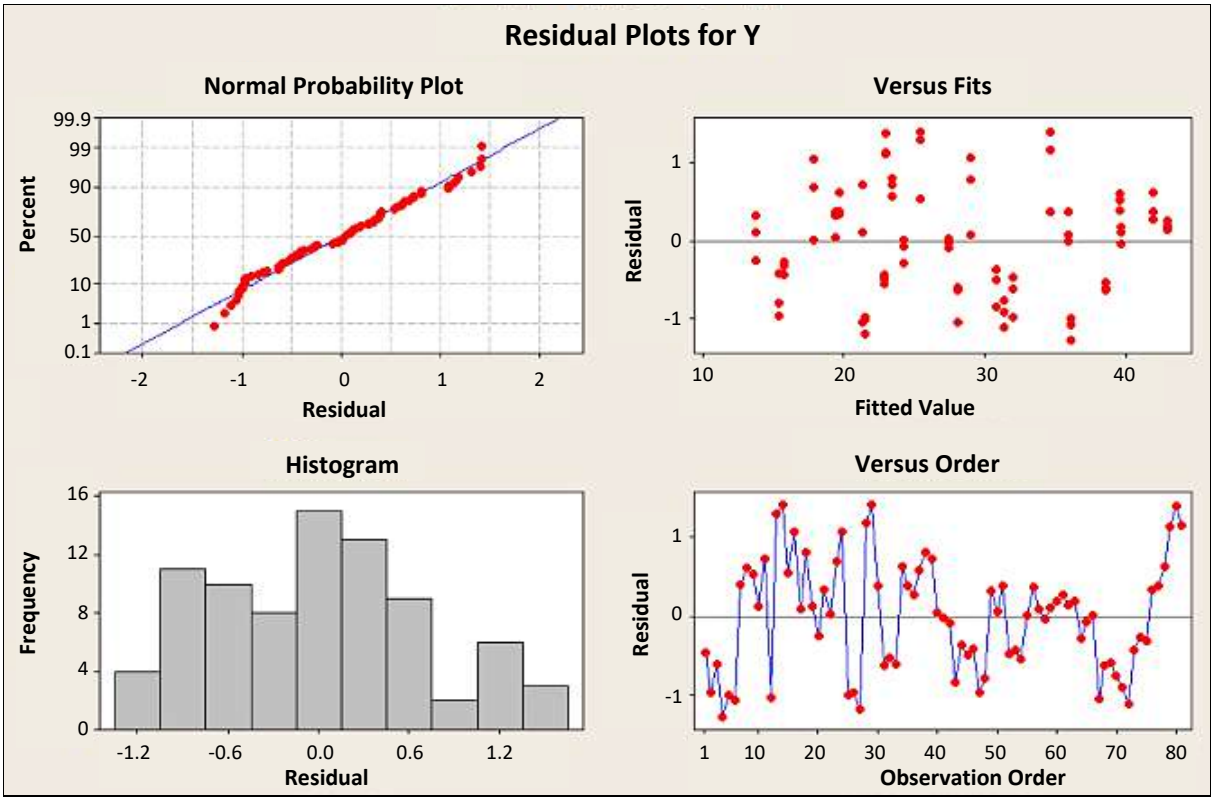

Figure 5 Analysing the accuracy of the experimental model

The experimental procedures included a verification of the accuracy and appropriateness of the data obtained. This was assessed through the probability plot of tensile strength, which yielded a P-value of 0.063. As the P-value is greater than the significance level ($\alpha = 0.05$), it indicates that the data follow a normal distribution. Examining Figure 5, which illustrates the normal probability plot of the residuals, further supports the normal distribution of the data. The histogram of the residuals also indicates a normal distribution. The residuals were examined in relation to the fitted values in the residuals versus the plot of the fitted values, revealing that the distribution of residuals did not exhibit a funnel or megaphone shape. Moreover, the test for independence of residuals, as shown in the residuals versus the order of the data plot, indicated that the residuals were independent of each other [27]. Therefore, it can be concluded that the experimental model, based on the full quadratic equation, is accurate and reliable.

Table 2 Results of Variance Analysis for the Full Quadratic Equation Model

Source	DF	Seq SS	Adj SS	Adj MS	F	P
Regression	9	1941.50	1941.50	215.72	371.16	0.000
Linear	3	1920.64	1920.64	640.21	1101.52	0.000
Square	3	17.87	17.87	5.96	10.25	0.000
Interaction	3	2.98	2.98	0.99	1.71	0.231
Residual Error	71	9.88	9.88	0.58		
Lack-of-Fit	3	34.66	34.66	21.9	02.04	0.128
Pure Error	54	5.02	5.02	0.09		
Total	80	5883.29				
R^2 = 99.33%; R^2(adj) = 99.24%						

From Table 2, the results of the variance for the full quadratic equation model reveal that the P-value of regression is 0.000, which is less than the predetermined confidence level (P-value < 0.05). Therefore, it can be concluded that the regression function in the full quadratic equation model has a linear nature, and the main factors significantly influence the response factors (print temperature (X_1), feed rate (X_2), and infill density (X_3)) at a 95% confidence level. When considering the adequacy of the model, the P-value for lack of fit is found to be 0.128, which is greater than 0.05 (P-value > 0.05). Hence, it can be concluded that the full quadratic equation model is adequate. The fitness of the model is further supported by an R-squared (R^2) value of 99.33% and an adjusted R-squared (R^2 adj) value of 99.24%, indicating reliable decision-making performance. The full quadratic equation model for predicting the tensile strength of 3D-printed objects is expressed in equation (6).

$$Y_{TS} = -17.2571 + 0.3833(X_1) - 0.1810(X_2) + 0.2679(X_3) - 0.0009(X_1^2) \\ -0.0008(X_2^2) + 0.0041(X_3^2) + 0.0003(X_1X_2) + 0.0012(X_1X_3) + 0.00002(X_2X_3) \quad (6)$$

The full quadratic equation model for predicting the tensile strength of 3D-printed objects has limitations on the input factors. The specified ranges for the input factors are as follows: print temperature (X_1) ranging from 190 to 230°C, feed rate (X_2) ranging from 30 to 70 mm/sec, and infill density (X_3) ranging from 40 to 80%. The output variable is denoted as *Y*, representing the tensile strength in MPa.

3.1.1 Main effect analysis

When examining hypotheses related to the impact of print temperature, feed rate, and infill density on tensile strength, as depicted in Figure 6, it becomes apparent that the primary effects of print temperature and infill density on tensile strength are observable. The results indicate that an increase in both print temperature and infill density leads to a corresponding increase in tensile strength. This trend aligns with findings from previous studies [28]. As for feed rate, the experimental results reveal a notable impact. A higher feed rate correlates with a decrease in tensile strength. This observation is consistent with the outcomes reported in the referenced research.

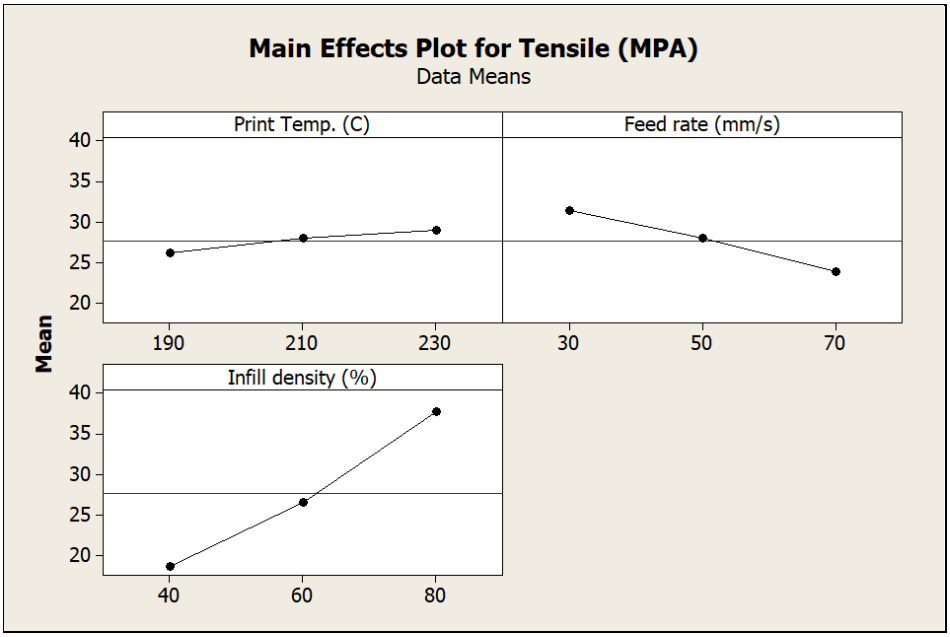

Figure 6 Relationship of main factors to tensile strength

3.1.2 Interaction effects

In testing the hypothesis of interaction effects among print temperature, feed rate, and infill density on tensile strength, as presented in Figure 7, it can be observed that the combined influence of print temperature with infill density, print temperature with feed rate, and feed rate with infill density does not have a significant impact on increasing the tensile strength of the printed components.

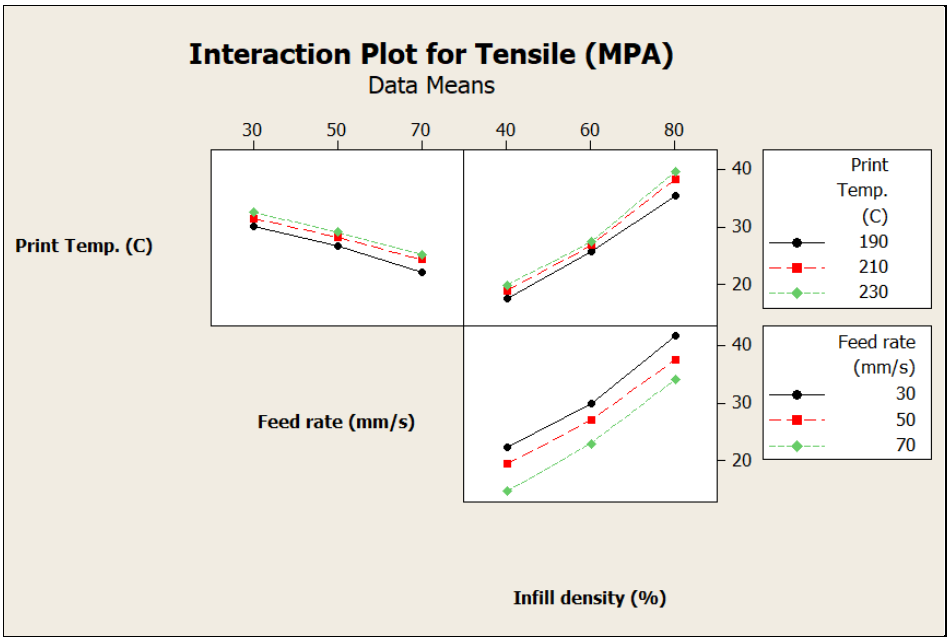

Figure 7 Interaction effects on tensile strength

3.1.3 Analysis of suitability for 3D printing of objects

The analysis of suitability for 3D printing of objects, considering tensile strength and the analysis of the microstructure, was conducted. This assessment aimed to determine the appropriateness of 3D printing for producing objects. The analysis utilised the surface response methodology, incorporating findings related to tensile strength and microstructure.

From Figures 8 and 9, it is evident that the surface response of the combined influences of the three factors on the tensile strength of 3D-printed objects reveals a correlation between infill density and print temperature. The reduction in tensile strength aligns with the increase in infill density and print temperature. Therefore, infill density and print temperature exhibit a relationship, where an increase in their values results in higher tensile strength. These influential factors are highlighted in the surface response. The optimal conditions for achieving the highest tensile strength, as indicated by the surface response, involve a print temperature(X_1) of 230°C, a feed rate (X_2) of 30 mm/sec, and an infill density (X_3) of 80%. Under these conditions, the tensile strength reaches a maximum value of 43.107 MPa, representing the most suitable state for 3D printing three-dimensional objects with the highest tensile strength.

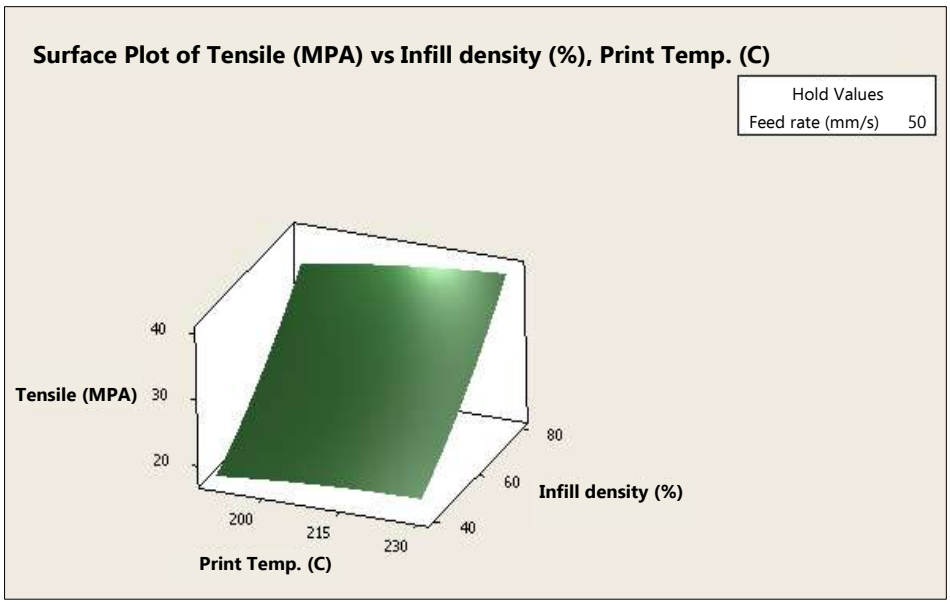

Figure 8 Surface response of combined influences - Infill density, Print temperature, and Feed rate

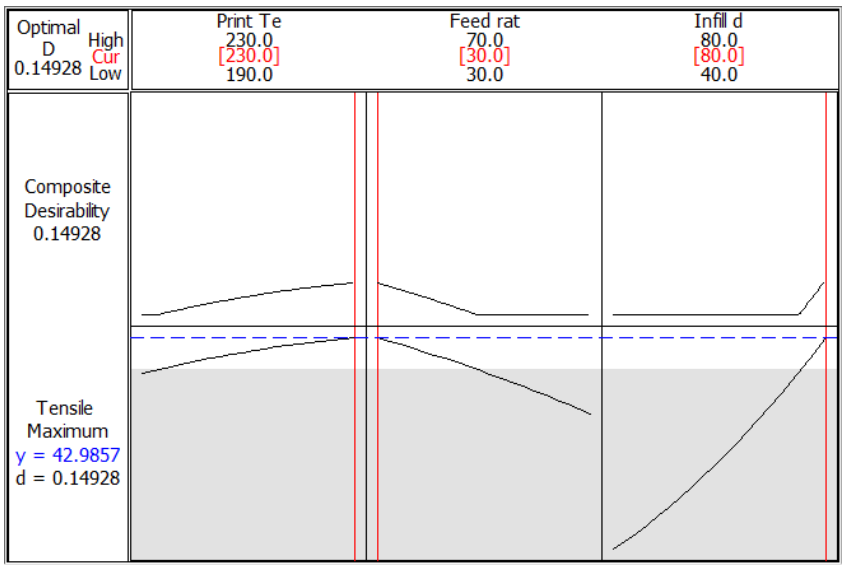

Figure 9 Suitability for 3D printing objects

3.2 Research results using neural network models

3.2.1 Data selection results for training and testing the system with K-fold Cross-Validation

In this study, K-fold cross-validation techniques were employed to thoroughly assess the efficiency of the data when utilised in training and testing artificial neural network models for predicting the tensile strength of 3D-printed objects. The dataset was divided into three equal subsets, each consisting of 27 data points. Two sets were utilised for the training process, while the remaining set was reserved for testing. The testing process was iterated three times, and the error values for each dataset are shown in Table 3.

Table 3 Results of Collecting Data with K-fold Cross-validation

k-fold Cross	Total mean square Error (MSE)
1	0.0227
2	**0.0154**
3	0.0262
Average	**0.0214**

The test results in Table 3 reveal that the dataset with the lowest total mean square error, amounting to 0.0154, corresponds to the second data subset. Consequently, this research opts to utilise the dataset from the second subset for both training and testing the neural network model.

3.2.2 Neural network architecture design for suitability

In this research, the design of the neural network architecture was conducted by specifying one layer with a total of six distinct configurations. Each configuration differed in the number of neurons in the layer. The selection of the suitable neural network architecture was based on the average mean square error (MSE) values, as depicted in Table 4.

Table 4 MSE Values for Neural Network Architecture Configurations

Neuron			MSE
Input Layer	**Hidden Layer**	**Output Layer**	
3	4	1	0.00149
3	8	1	0.00157
3	12	1	0.00148
3	**14**	**1**	**0.00133**
3	16	1	0.00155
3	20	1	0.00184
Average	0.018		

Based on the results in Table 4, the optimal neural network architecture for predicting the tensile strength of 3D-printed objects is determined to be 3-14-1. This architecture comprises 3 neurons in the input layer, 14 neurons in the hidden layer, and 1 neuron in the output layer. The learning algorithm employed is the Levenberg-Marquardt backpropagation. The activation functions used are logistic-sigmoid for the input layer, hyperbolic tangent-sigmoid for the hidden layer, and linear for the output layer. The generated neural network model demonstrated outstanding performance, achieving an average mean square error (MSE) of 0.00133. This underscores

the capability of the model to accurately predict the tensile strength of 3D-printed objects. The suitability of the architecture for this prediction task is demonstrated in Figure 10.

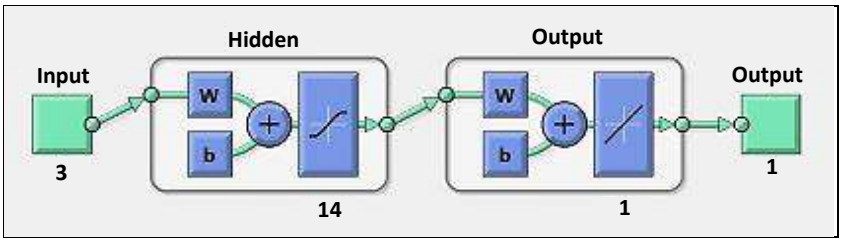

Figure 10 Neural network architecture for predicting tensile strength

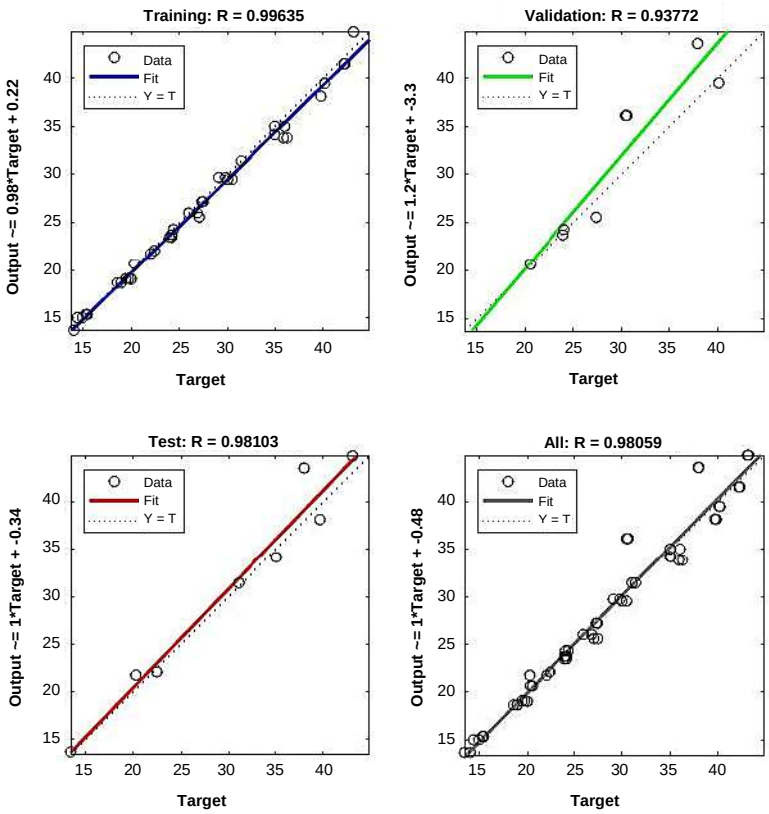

Figure 11 Relationship between target and predicted outputs

The results from the neural network model for predicting tensile strength, as shown in Figure 11, demonstrate high predictive performance. The decision-making efficiency metrics are as follows: 0.996 for learning, 0.981 for training, 0.938 for testing, and 0.981 for overall decision-making. The linear relationship is characterised by a slope of 1.0 and a y-intercept at 0.48. This linear correlation signifies a highly accurate relationship between the experimentally obtained target outputs and the outputs predicted by the neural network model. The model showcases strong efficiency and accuracy in predicting the tensile strength of 3D-printed objects.

3.3 Comparative results of model testing efficiency between neural network model and mathematical model

This section presents a comparison between the predictive capabilities of the mathematical model obtained from experimental surface response analysis and the neural network model for predicting the tensile strength of 3D-printed objects. The goal is to identify the model that provides precise predictions for tensile strength, with a focus on minimising the mean square error (MSE). This selection is crucial for practical applications to optimise the cost-effectiveness of 3D printing processes and enhance the overall performance of printed objects.

In Figure 12, the comparison between the predictions obtained from the neural network model and the target tensile strength values for 27 instances is depicted. The graph reveals that the values derived from the neural network model closely align with the target values. When evaluating the performance of the models, specifically comparing the neural network model with the full quadratic equation model, the average mean square error (MSE) for the neural network model is found to be 0.307. This is significantly lower than the average MSE from the full quadratic equation model, which is 1.392, as indicated in Table 5. Therefore, the neural network model demonstrates a remarkable capability to accurately predict the tensile strength values of 3D-printed objects.

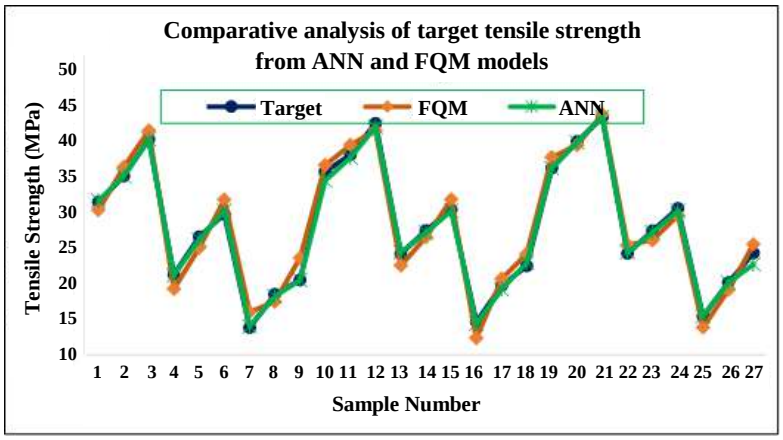

Figure 12 Comparative analysis of target tensile strength and predictions from neural network and full quadratic equation models

Table 5 Comparison of performance between the neural network model and the full quadratic model

No.	Printing Parameters			Tensile Strength Target	Tensile Strength Prediction			
	Print Temperature	Feed Rate	Infill Density		FQM	SE	ANN	SE
1	190	30	40	31.320	30.215	1.105	31.524	0.204
2	190	30	60	34.943	36.202	1.259	34.943	0.000
3	190	30	80	40.083	41.306	1.223	40.083	0.000
4	190	50	40	21.227	19.191	2.036	21.082	0.145
5	190	50	60	26.483	24.924	1.559	26.122	0.361
6	190	50	80	29.623	31.64	2.017	30.0867	0.464
7	190	70	40	13.751	15.979	2.228	13.962	0.211
8	190	70	60	18.453	17.425	1.028	18.140	0.313
9	190	70	80	20.444	23.52	3.076	20.444	0.000
10	210	30	40	35.593	36.48	0.887	34.323	1.27
11	210	30	60	37.927	39.281	1.354	37.543	0.384
12	210	30	80	42.312	41.35	0.962	41.833	0.479
13	210	50	40	24.107	22.477	1.63	24.342	0.235
14	210	50	60	27.357	26.401	0.956	27.053	0.306
15	210	50	80	30.242	31.687	1.445	30.087	0.155
16	210	70	40	14.613	12.342	2.271	14.355	0.258
17	190	70	60	19.634	20.607	0.973	19.123	0.511
18	190	70	80	22.390	24.111	1.721	22.859	0.469
19	230	30	40	36.064	37.57	1.506	36.064	0.000
20	230	30	60	39.763	39.269	0.494	39.651	0.112
21	230	30	80	43.107	43.589	0.482	43.235	0.128
22	230	50	40	24.123	25.351	1.228	24.270	0.147
23	230	50	60	27.318	25.986	1.332	27.090	0.228
24	230	50	80	30.442	29.445	0.997	30.086	0.356
25	230	70	40	15.367	13.813	1.554	15.354	0.013
26	230	70	60	20.054	19.032	1.022	20.054	0.000
27	230	70	80	24.177	25.414	1.237	22.625	1.552
						1.392		0.307

3.4 Microstructure investigations

Figure 13 shows SEM micrographs of the fracture surface of tensile specimens**.** On the other hand, Figure 14 reveals SEM micrographs of a cross-section of tensile specimens**.** In the FDM process, the 3D printer deposits filaments layer by layer, and these layers bond through local re-melting of previously solidified material. The specimens were manufactured under specific conditions, including an infill density of 80%, a feed rate of 30 mm/sec, and a print temperature of 230°C. These conditions resulted in specimens exhibiting good tensile strength and appealing exteriors. No flaws were observed on the exterior surfaces of these specimens. This suggests that specimens produced with less restrictive printing parameters probably had better adhesion between layers and deposited filaments. In other words, these sections displayed improved diffusion of polymer chains between layers, leading to denser sections with fewer interlayer spaces, consistent with the findings of previous research [29]. As the weak coalescence between layers made the interface more visible, some authors have noted that the layer thickness (LT) increases; printing fewer layers to complete the part may result in a less compact structure.

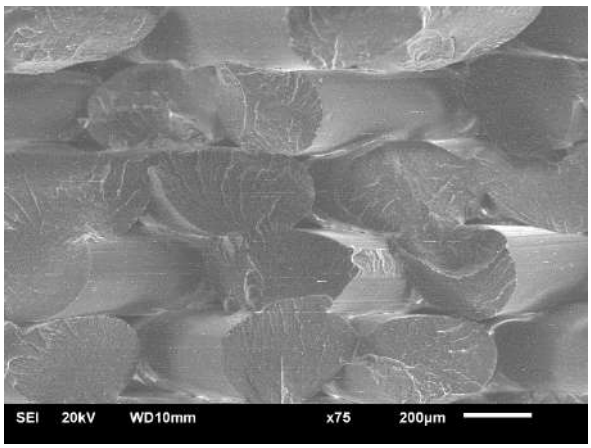

Figure 13 SEM image of the fracture surface of the tensile specimen with infill density = 80%, feed rate = 30 mm/sec, and print temperature = 230°C

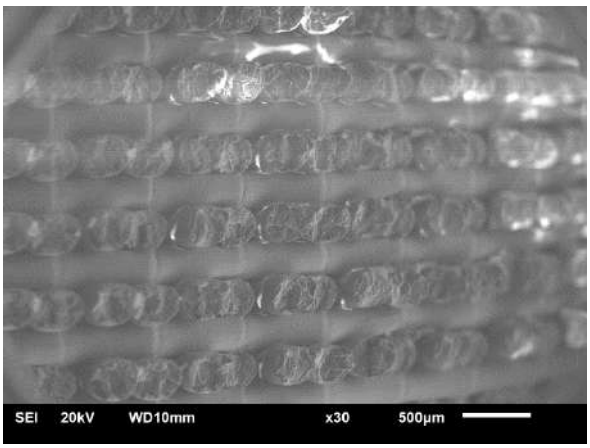

Figure 14 SEM image of the cross-section of a tensile specimen with infill density = 80%, feed rate = 30 mm/sec, and print temperature = 230°C

4. Discussion

The results of the tests on factors affecting 3D-printed objects indicate a trend of increasing tensile strength with higher print temperature and infill density. Conversely, an increase in feed rate leads to a decrease in tensile strength. Optimal conditions for producing three-dimensional objects with the highest tensile strength were identified as a print temperature of 230°C, a feed rate of 30 mm/sec, and an infill density of 80%. Under these conditions, the tensile strength reached a maximum value of 43.107 MPa. This outcome is attributed to the 3D printing process conducted at a high temperature and a low printing speed, resulting in uniform and well-adhered filaments in each layer of the print. Moreover, increasing the material infill leads to fewer internal voids in the structure of the object, promoting a tighter and more cohesive arrangement of filaments. Consequently, the tensile strength of the printed objects increases, aligning with previous research findings [30, 31]. A suitable neural network structure for predicting the tensile strength of 3D-printed objects has been identified as 3-14-1. This structure comprises 3 neurons in the input layer, representing the input features, 14 neurons in the hidden layer, and 1 neuron in the output layer, representing the predicted value. The neural network model achieved a minimum mean square error (MSE) of 0.00133. The network structure was deemed appropriate for predicting the tensile strength of 3D-printed objects, exhibiting a decision coefficient (R-squared) of 0.981 during testing. This indicates a high level of accuracy in the relationship between the target values obtained from experiments and the predictions made by the neural network model. The average MSE of the neural network model was found to be 0.307, lower than the average MSE of the full quadratic equation model, which was 1.392. This demonstrates that the neural network model can effectively predict the tensile strength of 3D-printed objects, providing accurate and efficient results.

5. Conclusions

The optimal printing parameters for achieving the highest tensile strength, as determined through Response Surface Methodology experiments, are a print temperature of 230°C, a feed rate of 30 mm/sec, and an infill density of 80%. Under these printing conditions, the test piece exhibited a maximum tensile strength resistance of 43.107 MPa. This was attributed to the even melting of the filaments, leading to better adhesion between layers during the printing process. Increasing infill density resulted in reduced internal voids within the structure of the printed object. This caused the filaments to adhere more tightly, enhancing the tensile strength resistance of the object. A neural network model was developed to predict the tensile strength resistance of printed objects based on three-dimensional printing parameters. The optimized neural network architecture consisted of three neurons in the input layer, 14 neurons in the hidden layer, and one neuron in the output layer (3-14-1). The learning process employed the Levenberg-Marquardt backpropagation algorithm with a mean squared error of 0.307, lower than the average error from the full quadratic model, which was 1.392. The suitable neural network structure, 3-14-1, demonstrated efficient decision-making with a decision coefficient of 0.938 for validation. The results of the neural network method obtained from this research will promote 3D printing in applications that require a focus on tensile properties. Manufacturers and researchers can apply it to forecasts. The attributes of 3D printed parts can be controlled with high quality and reliability, both to reduce production costs and increase efficiency in the 3D printing process. However, modelling with this neural network method still involves several limitations, such as requiring a large amount of data in training, and taking time to practice in order to obtain an accurate neural network model.

6. Acknowledgements

This research was supported by the Faculty of Engineering, Rajamangala University of Technology Krungthep and the Faculty of Science and Technology, Rajamangala University of Technology Srivijaya through the provision of facilities.

7. References

[1] Shahrubudin N, Lee TC, Ramlan R. An overview on 3D printing technology: technological, materials, and applications. Procedia Manuf. 2019;35:1286-96.

[2] Kaushik A, Garg RK. Tapping the potential of rapid prototyping techniques in creating a paradigm shift in the fabrication of occlusal splints. Rapid Prototyp J. 2023;29(10):2176-92.

[3] Kumar A, Chhabra D. Adopting additive manufacturing as a cleaner fabrication framework for topologically optimized orthotic devices: implications over sustainable rehabilitation. Clean Eng Technol. 2022;10:100559.
[4] Prater T, Werkheiser N, Ledbetter F, Timucin D, Wheeler K, Snyder M. 3D Printing in Zero G Technology Demonstration Mission: complete experimental results and summary of related material modelling efforts. Int J Adv Manuf Technol. 2019;101(1-4):391-417.
[5] Yadav D, Chhabra D, Gupta RK, Phogat A, Ahlawat A. Modelling and analysis of significant process parameters of FDM 3D printer using ANFIS. Mater Today Proc. 2020;21:1592-604.
[6] Mwema FM, Akinlabi ET. Basics of fused deposition modelling (FDM). In: Mwema FM, Akinlabi ET, editors. Fused deposition modelling: strategies for quality enhancement. Cham: Springer; 2020. p. 1-15.
[7] Sheoran AJ, Kumar H. Fused deposition modelling process parameters optimization and effect on mechanical properties and part quality: review and reflection on present research. Mater Today Proc. 2020;21:1659-72.
[8] Pandžić A, Hodžić D, Kadrić E. Experimental investigation on influence of infill density on tensile mechanical properties of different FDM 3D printed materials. TEM J. 2021;10(3):1195-201.
[9] Wankhede V, Jagetiya D, Joshi A, Chaudhari R. Experimental investigation of FDM process parameters using Taguchi analysis. Mater Today Proc. 2020;27:2117-20.
[10] Algarni M, Ghazali S. Comparative study of the sensitivity of PLA, ABS, PEEK, and PETG's mechanical properties to FDM printing process parameters. Crystals. 2021;11(8):995.
[11] Milovanović A. Sedmak A, Grbović A, Golubović Z, Mladenović G, Čolić K, et al. Comparative analysis of printing parameters effect on mechanical properties of natural PLA and advanced PLA-X material. Procedia Struct Integr. 2020;28:1963-8.
[12] Mamo HB, Tura AD, Santhosh AJ, Ashok N, Rao DK. Modelling and analysis of flexural strength with fuzzy logic technique for a fused deposition modelling ABS components. Mater Today Proc. 2022;57:768-74.
[13] Wang S, Ma Y, Deng Z, Zhang S, Cai J. Effects of fused deposition modelling process parameters on tensile, dynamic mechanical properties of 3D printed polylactic acid materials. Polym Test. 2020;86:106483.
[14] Akhavan-Safar A, Beygi R, Delzendehrooy F, da Silva LFM. Fracture energy assessment of adhesives—Part I: Is GIC an adhesive property? a neural network analysis. Proc Inst Mech Eng L: J Mater: Des Appl. 2021;235(6):1461-76.
[15] Delzendehrooy F, Beygi R, Akhavan-Safar A, da Silva LFM. Fracture energy assessment of adhesives Part II: Is GIIc an adhesive material property? (a neural network analysis). J Adv Join Process. 2021;3:100049.
[16] Yadav D, Chhabra D, Garg RK, Ahlawat A, Phogat A. Optimization of FDM 3D printing process parameters for multi-material using artificial neural network. Mater Today Proc. 2020;21:1583-91.
[17] Tura AD, Mamo HB, Jelila YD, Lemu HG. Experimental investigation and ANN prediction for part quality improvement of fused deposition modelling parts. IOP Conf Ser: Mater Sci Eng. 2021;1201:012031.
[18] Khan MS, Mishra SB. Minimising surface roughness of ABS-FDM build parts: an experimental approach. Mater Today Proc. 2020;26:1557-66.
[19] Kaushik A, Garg RK. Effect of printing parameters on the surface roughness and dimensional accuracy of digital light processing fabricated parts. J Mater Eng Perform. 2023:1-13.
[20] Kuznetsov VE, Solonin AN, Urzhumtsev OD, Schilling R, Tavitov AG. Strength of PLA components fabricated with fused deposition technology using a desktop 3D printer as a function of geometrical parameters of the process. Polymers. 2018;10(3):313.
[21] Dave HK, Prajapati AR, Rajpurohit SR, Patadiya NH, Raval HK. Investigation on tensile strength and failure modes of FDM printed part using in-house fabricated PLA filament. Adv Mater Process Technol. 2022;8(1):576-97.
[22] Pérez M, Medina-Sánchez G, García-Collado A, Gupta M, Carou D. Surface quality enhancement of fused deposition modelling (FDM) printed samples based on the selection of critical printing parameters. Materials. 2018;11(8):1382.
[23] Naveed N. Investigate the effects of process parameters on material properties and microstructural changes of 3D-printed specimens using fused deposition modelling (FDM). Mater Technol. 2021;36(5):317-30.
[24] Dong G, Wijaya G, Tang Y, Zhao YF. Optimising process parameters of fused deposition modelling by Taguchi method for the fabrication of lattice structures. Addit Manuf. 2018;19:62-72.
[25] ASTM. ASTM D638-14: Standard test methods for tensile properties of plastics. West Conshohocken: ASTM International; 2014.
[26] Goldberg Y. Neural network methods for natural language processing. Cham: Springer; 2017.
[27] Myers RH, Montgomery DC. Response surface methodology process and product optimization using designed experiments. 2nd ed. Hoboken: John Wiley and Sons; 2002.
[28] Naveed N. Investigating the material properties and microstructural changes of fused filament fabricated PLA and Tough-PLA parts. Polymers. 2021;13(9):1487.
[29] Moradi M, Aminzadeh A, Rahmatabadi D, Hakimi A. Experimental investigation on mechanical characterisation of 3D printed PLA produced by fused deposition modelling (FDM). Mater Res Express. 2021;8:035304.
[30] Vidakis N, Petousis M, Karapidakis E, Mountakis N, David C, Sagris D. Energy consumption versus strength in MEX 3D printing of polylactic acid. Adv Ind Manuf Eng. 2023;6:100119.
[31] Shirzad M, Zolfagharian A, Matbouei A, Bodaghi M. Design evaluation and optimization of 3D printed truss scaffolds for bone tissue engineering. J Mech Behav Biomed Mater. 2021;120:104594.